

MICRODOSIMETRIC STUDY AT THE CNAO ACTIVE-SCANNING CARBON-ION BEAM

P. Colautti^{1,*}, V. Conte¹, A. Selva¹, S. Chiriotti², A. Pola^{3,4}, D. Bortot^{3,4}, A. Fazzi^{3,4}, S. Agosteo^{3,4} and M. Ciocca⁵

¹INFN Laboratori Nazionali di Legnaro, Viale dell'Università 2, 35020 Legnaro, Italy

²Belgian Nuclear Research Centre, SCK•CEN, Boeretang 200, 2400 Mol, Belgium

³Politecnico di Milano, Dipartimento di Energia, via La Masa 34, 20156 Milano, Italy

⁴INFN, Sezione di Milano, via Celoria 16, 20133 Milano, Italy

⁵Fondazione CNAO, Strada Campeggi 53, 27100 Pavia, Italy

*Corresponding author: paolo.colautti@lnl.infn.it

The Italian National Centre for Oncological Hadrontherapy (CNAO) has been treating patients since 2011 with carbon-ion beams using the active-scanning modality. In such irradiation modality, the beam spot, which scans the treatment area, is characterised by very high particle-fluence rates (more than $10^5 \text{ s}^{-1} \text{ mm}^{-2}$). Moreover, the Bragg-peak is only $\sim 1 \text{ mm}$ -FWHM. Commercial tissue-equivalent proportional counters (TEPC), like the Far West Technologies LET- $\frac{1}{2}$, are large, hence they have limited capability to measure at high counting fluence rates. In this study we have used two home-made detectors, a mini-TEPC 0.81 mm^2 in sensitive area and a silicon telescope 0.125 mm^2 in sensitive area, to perform microdosimetric measurements in the therapeutic carbon-ion beam of CNAO. A monoenergetic carbon-ion beam of $189.5 \pm 0.3 \text{ MeV/u}$ scanning a $3 \times 3 \text{ cm}^2$ area has been used. Spectral differences are visible in the low y -value region, but the mean microdosimetric values, measured with the two detectors, result to be pretty consistent, as well as the microdosimetric spectra in the high y -value region.

INTRODUCTION

At present, there are 61 therapeutic centres worldwide that use particle beams to treat patients⁽¹⁾. Most of them use fast protons beams and 10 centres (three in Europe, five in Japan and two in China) use carbon ions. Beside the favourable physical properties, carbon ions offer biological advantages over protons: high relative-biological-effectiveness (RBE) and low oxygen-enhancement-ratio (OER)^(2, 3). The RBE enhancement and the OER lowering are related to linear-energy transfer (LET) increasing, as pointed out by several radiobiological studies performed at different LET values⁽⁴⁾. These features make carbon ions more suitable to treat tumours that are resistant to low-LET radiation. However, as a result of interactions with the target medium, the primary carbon-ion beam gives rise to a complex mixed radiation field⁽⁵⁾, the biological action of which varies inside the treated volume. Microdosimetric measurements can offer a valuable aid to characterise this complex radiation field and to assess RBE and OER values inside and outside the treatment volume, because of the similarity of microdosimetric mean values with mean LET values of the radiation field. Several microdosimetric measurements of carbon-ion beams have been performed in the past with tissue-equivalent proportional counters (TEPCs)⁽⁶⁻⁸⁾. Most of them have used the commercial Far West Technologies LET-1/2 spherical TEPC, which is a relatively large detector with a cross-section of 127 mm^2 (a sphere 12.7 mm in

diameter). However, up to now no microdosimetric measurements were performed in therapeutic beams using active-scanning modality, because of the high fluence rates, inside the pencil beam. To cope with high beam intensity of therapeutic ion beams, two mini detectors have been developed in the past: a mini-TEPC 0.81 mm^2 in geometrical cross-section⁽⁹⁾ and a silicon telescope⁽¹⁰⁾ of a sub-millimetric sensitive volume. The mini detectors have been used for the first time to measure at the active-scanning beam of the Italian National Centre for Oncological Hadrontherapy (CNAO). This study aims to check the consistency of microdosimetric data collected with the two detectors.

THE CNAO SCANNING BEAM

The CNAO clinical facility is equipped with a synchrotron capable of accelerating protons to kinetic energies in the range 60–250 MeV and carbon ions in the range 120–400 MeV/u⁽¹¹⁾. The carbon-ion pencil beam is extracted from the synchrotron approximately every 4.5 s. The extracted particle pulse lasts 1 s with an average intensity of $6 \times 10^7 \text{ s}^{-1}$, approximately. Such intensity can be reduced to 10% by using the F10 filter. The therapeutic beam quality does not change with the beam filter insertion. In this work a monoenergetic carbonion beam of 195.2 MeV/u was used. The Bragg peak was spread-out by using two thin PMMA ripple filters (2 mm in

thickness each). The emerging beam was calculated to have an average energy of 189.5 MeV/u and a FWHM (energy spread) of 0.28 MeV/u at the isocentre in air. The spot size FWHM was ~ 6 mm. The estimated fluence rate was $\sim 10^5 \text{ mm}^{-2} \text{ s}^{-1}$ at the isocentre, downstream of the F10 filter. The active-scanning system was used to irradiate uniformly a $3 \times 3 \text{ cm}^2$ surface. At each cycle the surface was irradiated with 225 equally spaced spots, and a sequence of 10 cycles was delivered to obtain a uniform absorbed dose of 10 Gy in water at the reference depth of 2 cm.

THE MINI-TEPC

The mini-TEPC has a cylindrical sensitive volume 0.9 mm in diameter and height, surrounded by a 0.35 mm-thick A-150-cathode wall, 0.35 mm Rexolite[®] insulator, a 0.2 mm-thick aluminium sleeve for a total external diameter of 2.7 mm. The detector stands inside the 160 mm long aluminium sleeve. The mini-TEPC works in gas-flow modality. The detector is connected with the gas line and the vacuum line through the Swagelok[®] quick connects, after positioning in the radiation field. The gas pressure inside the counter is maintained constant with Baratron[®] absolute manometers, a mass-flow controller, an electromagnetic solenoid valve and a control system (MKS Instruments). Individual pulses from the preamplifier are fed into a NIM/CAMAC/PC based data acquisition system for analogue and digital signal processing. Three spectroscopy linear amplifiers of different gains are used for shaping and amplifying simultaneously pulses from the preamplifier. Their shaping times have been set at 250 ns (the minimum allowed value with the used electronics) to minimise pulse pile-up. All the measurements were performed in gas-flow modality ($1 \text{ cm}^3 \text{ min}^{-1}$) at a pressure of 45 400 Pa of propane at 21.8°C in temperature; at that pressure the sensitive volume is equivalent to 1 μm site of C₃H₈-TE gas at density 1 g cm^{-3} ⁽¹²⁾.

Data processing

In order to minimise possible non-linear phenomena due to the high space-charge density occurring in the mini-TEPC for high gas gain and high-LET pulses, each microdosimetric spectrum was acquired in two separate runs: one measurement at low gas gain (mini-TEPC biased at 600 V) and the second one at higher gas gain (mini-TEPC biased at 750 V). The two parts of the spectrum have been joined off-line by matching the common spectral parts in the 90–110 keV/ μm region. The spectrum energy calibration has been performed by using the carbon-edge, i.e. the spectral region where the number of pulses per unit y -value drops sharply. The maximum electronic stopping-power value of carbon ions in

propane-TE is $988 \text{ keV } \mu\text{m}^{-1}$ (calculated with SRIM code⁽¹³⁾ at density 1 g cm^{-3}), thus giving $1482 \text{ keV } \mu\text{m}^{-1}$ by multiplying the LET value by 3/2. That value has been assigned to the carbon-edge intercept with the lineal energy axis. The lower detection threshold was $\sim 1 \text{ keV}/\mu\text{m}$. $f(y)$ spectra have been linearly extrapolated down to $0.1 \text{ keV}/\mu\text{m}$.

THE SILICON TELESCOPE

The silicon telescope is a pixelated detector consisting of a matrix of more than 7000 cylindrical ΔE elements (about $1.9 \mu\text{m}$ in thickness and $9 \mu\text{m}$ in diameter) coupled to a single residual-energy E stage ($500 \mu\text{m}$ in thickness)⁽¹⁰⁾. A silicon thickness of $1.9 \mu\text{m}$ is equivalent to $3.4 \mu\text{m}$ of propane-TE at density 1 g/cm^3 , according to the carbon-ion stopping-power mean ratio. Each ΔE element is surrounded by a guard-ring $14 \mu\text{m}$ in diameter that confines the charge collection within the lateral surface of the sensitive volume. The pitch among the elements is $\sim 41 \mu\text{m}$. In these measurements 1800 out of 7000 pixels have been connected in parallel to give an effective detection area of $\sim 0.125 \text{ mm}^2$. Both the ΔE and the E stages are biased and the respective signals are amplified and shaped by using two independent electronic chains. The electronic signals generated in the two stages are acquired by a two-channel ADC in coincidence mode.

Data processing

In these first measurements, only the ΔE signals have been used. Measured pulses were calibrated in terms of electronic charge injecting known amounts of charge through the preamplifier test input, the capacity of which is 4.7 pF. The charge pulses in the ΔE elements were collected, multiplied by 3.62 eV, divided by the electron charge and by the propane-TE-equivalent mean chord length of $2.27 \mu\text{m}$ ($2/3$ of $3.4 \mu\text{m}$) to obtain the lineal energy spectrum. The lower detection threshold was $\sim 10 \text{ keV}/\mu\text{m}$. $f(y)$ spectra have been linearly extrapolated down to $0.1 \text{ keV}/\mu\text{m}$.

THE IRRADIATION SETUP

Microdosimetric measurements were performed in one of the fixed horizontal beam lines at CNAO. The mini detectors were mounted vertically upside-down in a water phantom with the cylinder axis perpendicular to the beam line. The entrance window of the water phantom was placed at the isocentre of the treatment room and the central axis (depth-coordinate) of the phantom was aligned to match the beam axis. Detector holders could be moved along the beam axis with a precision of 0.1 mm. However, the position accuracy was not better than 0.6 mm,

because of the limited precision of the detector holder insertion in the phantom. The relative depth-dose profile of the ^{12}C beam was measured with an Advanced Markus chamber type PTW 34045. The absorbed dose in water under non-reference conditions for a $3 \times 3 \text{ cm}^2$ scanning field was measured following the formalism introduced in IAEA-TRS-398 Code of Practice⁽¹⁴⁾.

The dosimetric set up has a positioning uncertainty of 0.2 mm. The experimental uncertainty of the relative dose was estimated to be 0.3%. The microdosimeters were placed at different depths in the water phantom.

In Figure 1, the detector positions are marked on the relative dose profile.

EXPERIMENTAL RESULTS

Microdosimetric spectra acquired with the two detectors upstream and downstream of the Bragg peak are plotted together in Figures 2 and 3. By taking into account that the water-equivalent positions were not exactly the same, spectra of the two detectors look pretty similar, except in the low y -value region below the silicon-detector detection threshold of $10 \text{ keV}/\mu\text{m}$. The different equivalent site sizes ($1 \mu\text{m}$ for mini-TEPC and $3.4 \mu\text{m}$ for the silicon detector) do not play a significant role, since carbon ions are mainly crossers due to their high energy.

Microdosimetric spectra have been used to calculate the absorbed dose, D :

$$D = \frac{k}{\rho d^2} \cdot N \cdot \bar{y}_F$$

where, \bar{y}_F is the frequency-mean lineal energy, N the count number, d the site size, ρ the site density and k

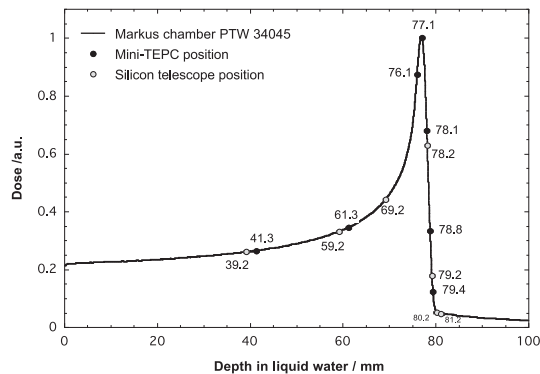


Figure 1. Detector positions are pointed out on the relative depth-dose curve.

a constant depending on the sensitive volume shape. The relative-dose values, measured with the two microdosimeters and with the ionisation chamber, are plotted in Figure 4. The ionisation chamber data are normalised to the Bragg peak value. Microdosimeter values are scaled to match the Markus chamber data at the shallowest depth in the proximal part of the Bragg peak. The position uncertainty was assessed to be 0.6 mm and the relative dose uncertainty 10%. The data consistency is satisfactory. However, further investigation has to be performed in order to reduce the absorbed dose uncertainty and hence response differences in the low y -value region.

Microdosimetric spectra have also been used to calculate the saturation-corrected dose-mean lineal energy y^* ⁽¹⁵⁾, a useful parameter to describe the beam quality in radiobiological track-experiments, for the two detectors:

$$y^* = y_0^2 \cdot \int [1 - e^{-(y/y_0)^2}] \cdot f(y) \cdot dy / \int y \cdot f(y) \cdot dy$$

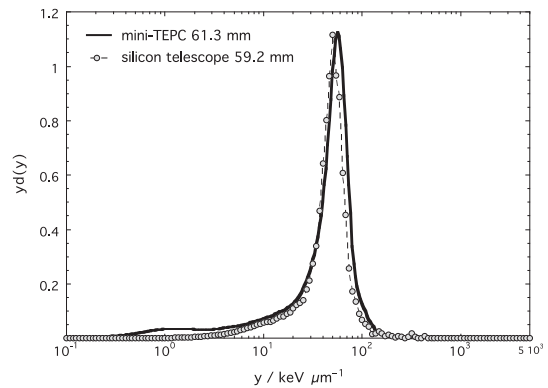


Figure 2. Microdosimetric spectra upstream of the proximal Bragg peak rise.

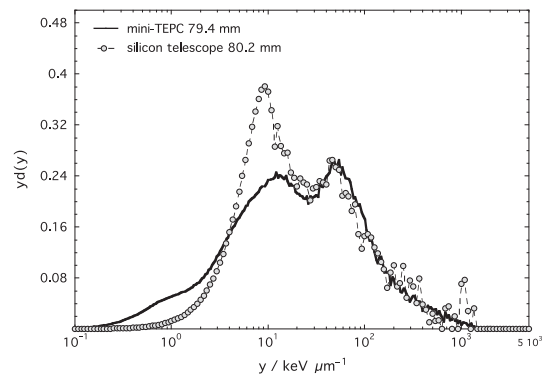


Figure 3. Microdosimetric spectra downstream of the distal Bragg peak.

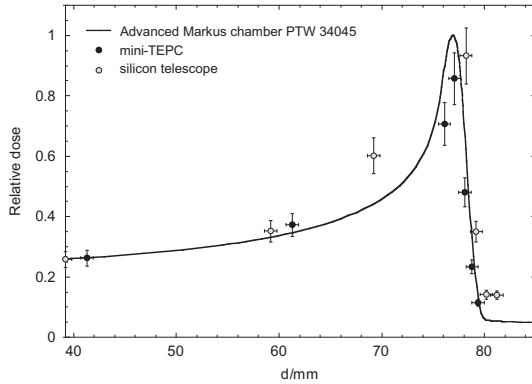


Figure 4. Relative dose measured with the two microdosimeters (see text) and with the ionisation chamber.

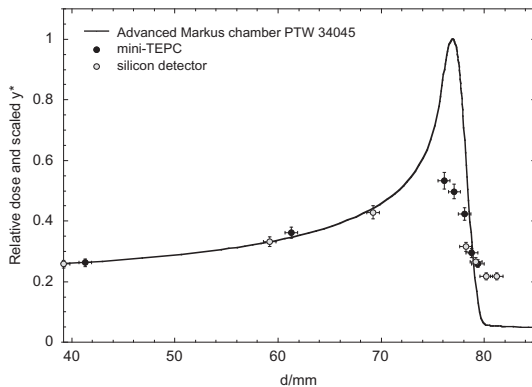


Figure 5. Relative dose and scaled saturation-corrected dose-mean lineal-energy (see text) at different water depths.

where, $y_o = 124 \text{ keV } \mu\text{m}^{-1}$ is an empirical saturation parameter for oxygenated cells⁽¹⁶⁾. To compare y^* variation with respect to dose variation against depth, y^* values have been scaled to match the Markus chamber values at the shallowest depths in the proximal part of the Bragg peak, see Figure 5. y^* uncertainty was assessed to be $\pm 5\%$. The absorbed dose at the Bragg peak resulted to be 3.8 times higher than in the proximal edge, while the y^* corresponding increase is 1.9. In the distal edge the y^* value decreases of a factor 2.5, but the decrease is smoother than the dose one. In spite of the simplified data processing of the silicon telescope, data of the two detectors are pretty consistent.

CONCLUSIONS

For the first time, the microdosimetric features of the CNAO active-scanning ^{12}C beam have been studied. Two microdosimeters have been used: a mini tissue-

equivalent gas-proportional counter and a silicon detector. The two detectors are different in terms of composition, data acquisition and data processing. However, their measurements of relative dose and relative y^* at different depths give consistent results. Microdosimetric spectra of the two detectors show significant differences in the low y -value region. However, these differences and the different equivalent sizes seem to play a minor role when the relative absorbed dose and the relative y^* are calculated. These first measurements are encouraging, suggesting microdosimetric measurements are reliable and reproducible also for carbon-ion active-scanning beams, although further measurements are still necessary to reduce experimental uncertainties and to improve the data collection accuracy.

FUNDING

This research was supported by INFN with the contract MITRA of the V Scientific Commission.

REFERENCES

1. PTCOG 2016. *Hadrontherapy Facilities Worldwide in Operation*. www.ptcog.ch (updated 05-April 2016).
2. Raju, M. R., Amols, H. I., Bain, E., Carpenter, S. G., Cox, R. A. and Robertson, J. B. *A heavy particle comparative study. Part III. OER and RBE*. Br. J. Radiol. **51**, 712–719 (1978).
3. Curtis, S. B. *The OER of mixed high- and low-LET radiation*. Radiat. Res. **65**, 566–572 (1976).
4. Singers Sørensen, B., Overgaard, J. and Bassler, N. *In vitro RBE-LET dependence for multiple particle types*. Acta Oncol. (Madr.) **50**, 757–762 (2011).
5. Gunzert-Marx, K., Iwasw, H., Schrdt, D. and Simon, R. S. *Secondary beam fragments produced by 200 MeV u^{-1} ^{12}C ionsing water and their dose contributions in carbon ion therapy*. New J. Phys. **10**, 075003 (2008).
6. Kase, Y., Kanai, T., Sakama, M., Tameshige, Y., Himukai, T., Nose, H. and Matsufuji, N. *Microdosimetric approach to NIRS-defined biological dose measurements for carbon-ion treatment beam*. J. Radiat. Res. **52**, 59–68 (2011).
7. Endo, S., Tanaka, K., Ishikawa, M., Hoshi, M., Onizuka, Y., Takada, M., Yamaguchi, H., Hayabuchi, N., Maeda, N. and Shizuma, K. *Microdosimetric evaluation of the 400 MeV/nucleon carbon beam at HIMAC*. Med. Phys. **32**, 3843–3848 (2010).
8. Martino, G., Durante, M. and Schardt, D. *Microdosimetry measurements characterizing the radiation fields of 300 MeV/u ^{12}C and 185 MeV/u ^7Li pencil beams stopping power in water*. Phys. Med. Biol. **55**, 3441–3449 (2010).
9. De Nardo, L., Cesari, V., Donà, G., Magrin, G., Colautti, P., Conte, V. and Tornielli, G. *Mini-TEPCs for radiation therapy*. Radiat. Prot. Dosim. **108**, 345–352 (2004).
10. Agosteo, S., Fallica, P. G., Fazzi, A., Introini, M. V., Pola, A. and Valvoc, G. *A pixelated silicon telescope for solid state microdosimetry*. Radiat. Meas. **43**, 585–589 (2008).
11. Mirandola, A. *et al.* *Dosimetric commissioning and quality assurance of scanned ion beams at the Italian*

- National Centre for Oncological Hadrontherapy*. Med. Phys. **42**, 5287–5300 (2015) doi:10.1118/1.4928397.
12. Chiriotti, S., Moro, M., Colautti, P., Conte, V. and Grosswendt, B. *Equivalence of pure propane and propane-TE gases for microdosimetric measurements*. Radiat. Prot. Dosim. **166**, 242–246 (2015).
 13. Ziegler, J. F., Ziegler, M. D. and Biersack, J. P. *SRIM The stopping and range of ions in matter*. Nucl. Instrum. Methods **B268**, 818–1823 (2010).
 14. IAEA-TRS-398. *Absorbed dose determination in external beam radiotherapy: an international code of practice for dosimetry based on standards of absorbed dose to water*. In: IAEA Technical Report, vol. 398 (2005).
 15. International Commission on Radiation Units and Measurements. *Microdosimetry*. ICRU report 36 (1983).
 16. Kellerer, A. M. and Rossi, H. H. *The theory of dual radiation action*. Curr. Top. Radiat. Res. **8**, 85–158 (1972).